Significant Enhancement of Neutralino Dark Matter Annihilation
from Electroweak Bremsstrahlung

Torsten Bringmann[*]

*Department of Physics, University of Oslo, Box 1048, NO-0316 Oslo, Norway and II. Institute for Theoretical Physics,
University of Hamburg, Luruper Chaussee 149, DE-22761 Hamburg, Germany*

Francesca Calore[†]

*GRAPPA Institute, University of Amsterdam, Science Park 904, 1090 GL Amsterdam, The Netherlands
and II. Institute for Theoretical Physics, University of Hamburg, Luruper Chaussee 149, DE-22761 Hamburg, Germany*

(Received 27 September 2013; published 19 February 2014)

Indirect searches for the cosmological dark matter have become ever more competitive during the past years. Here, we report the first full calculation of leading electroweak corrections to the annihilation rate of supersymmetric neutralino dark matter. We find that these corrections can be huge, partially due to contributions that have been overlooked so far. Our results imply a significantly enhanced discovery potential of this well motivated dark matter candidate with current and upcoming cosmic ray experiments, in particular for gamma rays and models with somewhat small annihilation rates at the tree level.

Introduction.—Thermally produced weakly interacting massive particles (WIMPs) constitute a prime candidate for the so far unexplained cosmological dark matter (DM), with the lightest supersymmetric neutralino, henceforth denoted by χ, being one of the best motivated and most often studied examples [1]. Indirect searches for WIMP DM, looking for DM annihilation products in the galactic halo or at cosmological distances, are putting ever more stringent constraints on the annihilation rate, and operating or upcoming experiments like Fermi [2], AMS [3], or CTA [4] are expected to explore a large part of the remaining parameter space of viable models. Because of their outstanding constraining and signal identification power, gamma rays have been argued to be the "golden channel" of indirect searches (see Ref. [5] for a recent review), and this is what we will mostly focus on here.

In view of the small galactic velocities $v \sim 10^{-3}$ of DM particles, there is little hope for such experiments to be sensitive to anything but s-wave annihilation. For Majorana particles like the neutralino, however, the annihilation into fermionic two-body states $\bar{f}f$ is helicity suppressed in the $v \to 0$ limit, by a factor of m_f^2/m_χ^2, because the incoming DM particle pair forms a $J = 0$ state [6]. This suppression can be avoided in the presence of an additional photon in the final state, in particular, if emitted from a virtual sfermion with a mass close to m_χ [7,8]. The radiative "correction," thus, becomes parametrically as large as $\alpha_{em}/\pi(m_\chi^2/m_f^2)$, implying an annihilation into $\bar{f}f\gamma$ final states at a rate up to several orders of magnitude above the tree-level result. Of course, the same mechanism also works for the emission of other vector bosons and, thus, has been intensely studied in the context of indirect DM searches not only for photons [9–18], but also for electroweak gauge

bosons [19–27] and gluons [28,29] (see Ref. [30] for a recent general analysis).

Phenomenologically, the most important characteristics of photon "internal bremsstrahlung" (IB) [10] are the associated pronounced spectral features in gamma rays that can appear near the highest kinematically accessible energies (notably, not only for fermion, but also for W^+W^- final states [31,32]). Such gamma-ray features can help tremendously to both detect a DM signal and to distinguish it from astrophysical backgrounds [12,33].

Electroweak or strong gauge boson IB, on the other hand, generically proceeds at considerably higher rates due to the larger coupling strength involved. As a result of the decay and fragmentation of the additional gauge boson, however, it affects the gamma-ray spectrum only at energies much below the DM mass and does not introduce any pronounced spectral features. The potentially large enhancement can still be very important for photon (or other cosmic ray) counting experiments with low energy thresholds. It was also pointed out that electroweak IB can be phenomenologically important even when not lifting the helicity suppression, like for final state radiation, because it may significantly alter the composition of the DM-induced cosmic-ray spectrum [34–37].

Encouraged by the importance of an additional W/Z boson in fermion final states as found in previous studies, we present here the first fully general calculation for neutralino DM, keeping not only all relevant diagrams, but also the full mass dependence of both fermions and gauge bosons. We identify new enhancement mechanisms and show that model-independent results [37,38], though being quite popular, are in general not sufficient to produce realistic estimates of DM indirect detection prospects.

Neutralino annihilation into fermions and Z/W±.—
In the minimal supersymmetric standard model (MSSM),
the lightest neutralino is a linear combination of the neutral
superpartners of the gauge and Higgs fields, $\chi \equiv \chi_1^0 =$
$N_{11}\tilde{B} + N_{12}\tilde{W}^3 + N_{13}\tilde{H}_1^0 + N_{14}\tilde{H}_2^0$, with $Z_g \equiv |N_{11}|^2 +$
$|N_{12}|^2$ indicating its gaugino fraction. We collect in
Fig. 1, in a very condensed form, all Feynman diagrams
that contribute to neutralino annihilation into two fermions
and one $SU(2)$ gauge boson, in total 46 for $W^\pm$ and 88 for
Z emission, where dotted lines indicate scalar (A, h, H, and
$H^\pm$) or vector (Z, $W^\pm$) mediators. Diagrams in the first
(second) row derive from tree-level s-(t-) channel diagrams;
u-channel derivates are not shown explicitly and for $v \to 0$
simply result in the same amplitudes as the t-channel case.
For each tree-level topology, the diagrams can further
loosely be classified by whether the electroweak gauge
boson is radiated from the virtual particle that appears at tree
level [virtual internal bremsstrahlung (VIB), first column],
one of the final fermions [final state radiation (FSR), second
and third columns], or by one of the initial neutralino legs
[initial state radiation (ISR), columns 4 and 5].

We generate those diagrams with FEYNARTS [39],
modifying the supplied generic MSSM model file such
as to agree with the conventions adopted in DARKSUSY
[40], and use FEYNCALC [41] to calculate the amplitudes.
In order to obtain tractable analytic expressions, we restrict
ourselves to the $v \to 0$ limit, in which only the singlet state
($J^P = 0^-$) of the neutralino pair contributes; in practice,
we replace the pair of external Majorana spinors in the
amplitude by the Lorentz-invariant projector $P_{1_{S_0}} =$
$(\gamma_5/\sqrt{2})(m_\chi - \not{p}/2)$, where p is the total momentum of
the system. In the next step, we adapt the helicity amplitude
method which has proven very useful for the numerical
analysis of neutralino annihilation into two-body final
states [42,43] to our case. Concretely, we compute the
total amplitude squared, summed over final and averaged
over initial spin degrees of freedom, as

$$\overline{|\mathcal{M}|^2} = \frac{1}{4}\sum_{h,\lambda}|\sum_{\text{diag.}}\mathcal{M}^{(h,\lambda)}_{\chi\chi\to\bar{F}fV}|^2. \qquad (1)$$

Here, h refers to the helicity of the fermion-antifermion pair
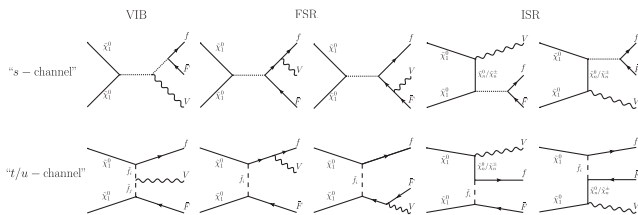in its rest frame [where F equals f for $V = Z$, while for

FIG. 1.   Condensed representation of all Feynman diagrams for
$\chi\chi \to \bar{F}fV$, where $F = f$ for Z-boson emission ($V = Z$) and (F,
f) are the two components of an $SU(2)_L$ doublet for W-boson
emission ($V = W^\pm$). Dotted lines indicate scalar (A, h, H, $H^\pm$) or
vector (Z, $W^\pm$) mediators.

$V = W^\pm$ it is given by its $SU(2)_L$ partner], λ is the
polarization state of V in the same system and the inner
sum runs over all diagrams of Fig. 1 (for more technical
details, see Ref. [44]). Finally, the cross section is obtained
by integration over the three-body phase space

$$\frac{d(\sigma v)}{dE_1 dE_2} = \frac{1}{16m_\chi^2}\frac{1}{(2\pi)^3}\overline{|\mathcal{M}|^2}, \qquad (2)$$

where E_1 and E_2 are the center-of-mass system (c.m.s.)
energies of any two final state particles.

As a cross-check of our results, we analytically repro-
duced the differential cross section for $\chi\chi \to \bar{f}f\gamma$ [10], for
all diagrams and $m_f \neq 0$, by taking the appropriate limit
of our expressions for $\bar{f}fZ$ final states. We also find exact
agreement for $\bar{f}fZ$ and $\bar{F}fW$ final states in the limits
considered in Ref. [30], which extends earlier partial results
for those processes [19,20,23], i.e., $m_f \equiv 0$ and χ being a
pure Bino or Higgsino. Compared to those references,
however, our expressions are considerably more complex
because we keep the full mass dependence as well as the
much larger number of diagrams that appear for mixed
neutralinos. All matrix elements and cross sections have
been implemented in DARKSUSY and will be available
with the next public release.

Spectra of stable annihilation products.—Integration of
Eq. (2) directly gives the spectrum of any of the final state
particles p—which, however, mostly fragment or decay.
The spectrum of a potentially observable stable particle P,
resulting from a given annihilation channel $\chi\chi \to \bar{F}fV$ and
normalized to the total tree-level annihilation rate σv_0^{tot}, can
be written as

$$\frac{dN_P^{\bar{F}fV}}{dE_P} = \sum_{p=F,f,V}\int_{E_p^{\min}}^{E_p^{\max}}\frac{1}{2}\frac{dN_P^{\bar{p}p\to P+X}}{dE_P}\frac{dN_p^{\bar{F}fV}}{dE_p}dE_p, \qquad (3)$$

where

$$\frac{dN_p^{\bar{F}fV}}{dE_p} = \frac{1}{\sigma v_0^{\text{tot}}}\int_{E_{p'}^{\min}(E_p)}^{E_{p'}^{\max}(E_p)}\frac{d(\sigma v)}{dE_p dE_{p'}}dE_{p'} \qquad (4)$$

and $dN_P^{\bar{p}p\to P+X}/dE_P$ is the Monte Carlo (MC) simulated
number of stable particles P resulting from the inclusive
process $\bar{p}p \to P + X$ (evaluated for a c.m.s. energy of
$2E_p$). Those MC spectra are implemented in DARKSUSY,
based on a large number of PYTHIA [45] runs. They have a
strong and characteristic dependence on the fractional
c.m.s. energy $x_P \equiv E_P/E_p$ carried by the stable particle
P (while the dependence on the energy scale E_p itself is
rather weak, at least for $E_p \gg m_p$). The total photon yield
from the $SU(2)$ corrections reported here, e.g., is, thus,
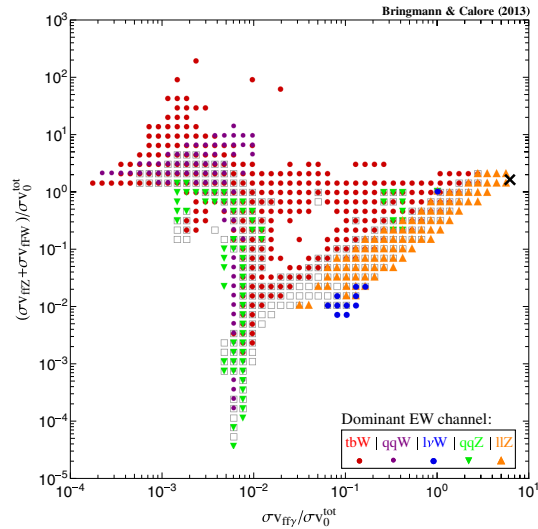given by the sum over all final states $\bar{F}fV$

FIG. 2 (color online). Total annihilation cross section of thermally produced neutralino DM, in the CMSSM and MSSM-7, into any fermion pair and a photon (with $E_\gamma > 0.5m_\chi$) or an electroweak gauge boson, divided by the total cross section at tree level. The dominant $SU(2)$ annihilation channel is also indicated, with q being any quark but the top (note that $\bar{t}tZ$ never dominates; empty squares correspond to models where no single channel contributes more than 50%). The black cross marks the example model given in Table I.

$$\frac{dN_\gamma^{SU(2)}}{dE_\gamma}(E_\gamma) = \sum_{i \in \{\bar{F}fV\}} \frac{dN_\gamma^i}{dE_\gamma}(E_\gamma). \qquad (5)$$

Parameter scan and cross section results.—In order to illustrate the potential importance of the processes calculated here, we consider an extensive scan over the parameter space of the constrained MSSM (CMSSM) and a phenomenological MSSM-7 (see Ref. [5] for details), where we only keep those $\sim 4 \times 10^5$ models with a neutralino relic density within the 3σ estimate of Planck [46]. In Fig. 2, we compare the total annihilation rate into three-body final states including a fermion pair and an electroweak gauge boson with that for $\bar{f}f\gamma$ final states, indicating also the dominant $SU(2)$ annihilation channel [47].

The first thing to notice is that electroweak corrections can be quite a bit larger than electromagnetic corrections, and that the correlation between those two is generally not all too pronounced. The reason for this can be found in the much larger number of diagrams that are involved, which results in a rich and complex phenomenology. A full discussion is beyond the scope of this Letter and will be presented elsewhere [44], but in the following, we will point out the main enhancement mechanisms that result in the structure visible in Fig. 2.

The only case where there is actually a clear correlation between the two IB contributions is the pronounced orange strip with $\ell^+\ell^-Z$ final states dominating the electroweak IB. Those models—as well as those dominated by $\ell^\pm\nu W^\mp$—mostly lie in the CMSSM stau coannihilation
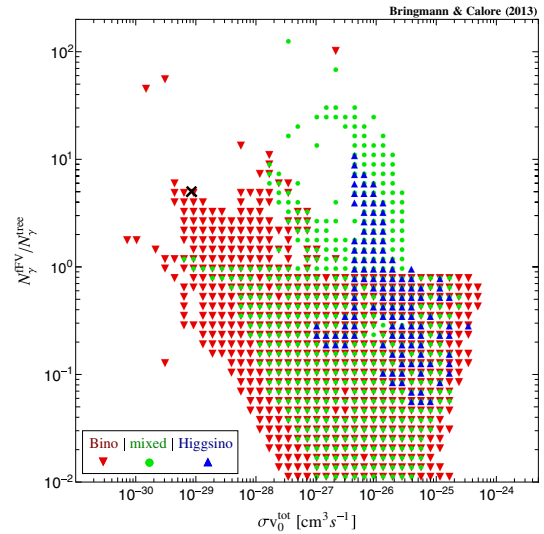

FIG. 3 (color online). Photon yield enhancement (for $E_\gamma > 100$ MeV) from neutralino DM annihilation due to electroweak radiative corrections vs the full annihilation rate σv_0^{tot} at the tree level (in the CMSSM and MSSM-7). Symbols indicate models where the neutralino is mostly Bino ($Z_g > 0.99$), Higgsino ($Z_g < 0.01$), or mixed ($0.01 \leq Z_g \leq 0.99$). The black cross marks the example model given in Table I.

region, where the mass degeneracy between sleptons and the neutralino results in a well-known strong enhancement of t-channel VIB diagrams [10,11,21,22,30] (somewhat suppressed in the electroweak case due to destructive interference with s-channel diagrams). The vertical strip with dominantly $\bar{q}qZ$ final states mostly corresponds to Binos resonantly annihilating via s-channel A exchange. FSR cannot lift the helicity suppression here, which explains the smallness of the $U(1)$ contributions; moving up the strip, the neutralinos feature an increasing Higgsino fraction—which opens up the ISR channels and, thus, potentially large enhancement factors due to a lifting of the helicity suppression [24].

The largest enhancements appear for tbW final states (note that qqW only dominates for $2m_\chi \lesssim m_t + m_W$), due to various reasons. One of the strongest enhancement mechanisms that we identified is a threshold effect [48–50] for $m_\chi \lesssim m_t$, where $\bar{t}t$ final states are kinematically not allowed or strongly suppressed. Resonances can also play an important role for some models, as well as the fact that the s-channel amplitude is directly proportional to the large top mass.

Implications for DM searches.—For indirect DM detection, a more suitable measure for the impact of the radiative corrections reported here is the enhancement of cosmic ray yields at low energies. In Fig. 3, we show this quantity for photons with $E_\gamma > 100$ MeV (roughly the threshold of Fermi). The photon count can be enhanced by up to 2 orders of magnitude, in particular for models where the total annihilation rate at tree level is smaller than the "canonical" value of $\langle \sigma v \rangle_{therm} \equiv 3 \times 10^{-26}$ cm^3 s^{-1} for thermally produced DM. Comparing this to the model-independent limits derived from three years of dwarf galaxy

observations [51], we find that even some thermally produced neutralinos as heavy as several hundred GeV could eventually be probed by Fermi once electroweak corrections are taken into account [52].

Even when increasing the energy threshold to $E_{thr} \sim 100$ GeV, as is typical for currently operating air Cherenkov telescopes, the resulting enhancement in the photon flux is very sizable—not the least because particularly large effects can be found for DM masses in the TeV range (in which case one has $m_\chi \gg E_{thr}$, implying that the photon yield enhancement is very similar to the one shown in Fig. 3 for $E_{thr} = 0.1$ GeV). Given its lower targeted threshold, radiative corrections will obviously be even more important when interpreting the results of DM searches with CTA. While we have limited the above discussion to gamma rays, we note that corresponding considerations apply to other cosmic ray species [44]. In particular, electroweak corrections can completely dominate the neutrino signal [26,27] and prospects for indirect DM searches with antiprotons or positrons through the AMS experiment can be improved significantly (especially, as expected [53], for light neutralinos).

It is worth mentioning that elastic scattering rates are rather uncorrelated with the three-body cross sections calculated here; in particular, we checked that including the most recent direct detection bounds [54] does not qualitatively change Figs. 2 or 3. While such a correlation is also absent at tree level [55], it may, in contrast, be quite strong when considering, instead, electromagnetic corrections in models with very small mass differences between squarks and neutralinos [15] (because in this case the zero photon mass and the absence of destructively interfering s-channel diagrams lead to an unsuppressed enhancement).

Last, but not least, we illustrate, in Fig. 4, how the spectral shape of gamma rays from DM annihilation can be distorted when including electroweak corrections. The example shown here corresponds to a typical Bino-like CMSSM model in the $\tilde\tau$-coannihilation region, with model

TABLE I.   CMSSM model parameters for the spectrum shown in Fig. 4, along with neutralino mass m_χ, gaugino fraction Z_g, mass of the lightest stau $m_{\tilde\tau}$, and relic density Ωh^2.

m_0 [GeV]	$m_{1/2}$ [GeV]	$\tan\beta$	A_0 [GeV]	sgn (μ)	m_χ [GeV]	Z_g	$m_{\tilde\tau}$ [GeV]	Ωh^2
168	871	4.61	−292	−1	362.5	0.999	364.3	0.113

parameters as specified in Table I and satisfying current LHC limits on the squark and gluino masses [56,57]. As expected, the effect of electroweak corrections results in a rather featureless spectrum and is mostly seen at relatively low photon energies (while electromagnetic corrections produce a sharp spectral feature at high $E_\gamma \sim m_\chi$). However, electroweak IB certainly induces a very sizable change of both total photon flux and spectral form. In particular, it is worth stressing that this is almost completely due to the full calculation presented here: using instead, the often adopted model-independent expressions for FSR [37]—as implemented, e.g., in Ref. [38]—results in a total photon flux for this model that is essentially indistinguishable from the tree-level result (dashed line).

Conclusions.—We have performed a full calculation of leading electroweak corrections to the annihilation cross section of supersymmetric neutralino DM, demonstrating that such corrections may significantly enhance the annihilation rate of WIMP DM in realistic particle physics frameworks. While these processes do not produce pronounced spectral features in gamma rays like the corresponding electromagnetic corrections, they may—depending on the detector threshold—enhance the observationally also highly relevant integrated photon yield by up to 2 orders of magnitude compared to the tree-level expectation.

Let us stress that previous results available in the literature, concerning both "model-independent" parametrizations of the photon yield [37,38] and analytic results under various limiting assumptions [19,20,22–25,30], are in many situations not reliable enough to reproduce be it the shape or the normalization of the gamma-ray spectrum. This clearly illustrates the need for detailed calculations as presented here, which we are convinced will prove important for future indirect DM searches. We refer to a companion paper [44] for a more detailed discussion, including implications for indirect DM searches with other cosmic ray species. The routines to compute the processes discussed here will be fully available with the next public DARKSUSY release.
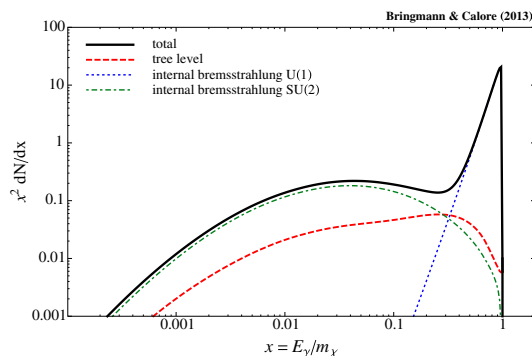
FIG. 4 (color online).   Gamma-ray spectrum from neutralino DM annihilation for the example model of Table I (solid line). Shown separately is the tree-level annihilation spectrum (dashed line), the spectrum from electroweak corrections only (computed in this Letter, dashed-dotted line) and from electromagnetic corrections only (following Ref. [10], dotted line).

[1] G. Jungman, M. Kamionkowski, and K. Griest, Phys. Rep. **267**, 195 (1996).

[2] W. B. Atwood *et al.* (LAT Collaboration), Astrophys. J. **697**, 1071 (2009).

[3] R. Battiston, M. Biasini, E. Fiandrini, J. Petrakis, and M. H. Salamon, Astropart. Phys. **13**, 51 (2000).

[4] M. Doro *et al.* (CTA Collaboration), Astropart. Phys. **43**, 189 (2013).

[5] T. Bringmann and C. Weniger, Phys. Dark Univ. **1**, 194 (2012).

[6] H. Goldberg, Phys. Rev. Lett. **50**, 1419 (1983); **103**, 099905 (E) (2009).

[7] L. Bergström, Phys. Lett. B **225**, 372 (1989).

[8] R. Flores, K. A. Olive, and S. Rudaz, Phys. Lett. B **232**, 377 (1989).

[9] E. A. Baltz and L. Bergström, Phys. Rev. D **67**, 043516 (2003).

[10] T. Bringmann, L. Bergström, and J. Edsjö, J. High Energy Phys. 01 (**2008**) 049.

[11] L. Bergström, T. Bringmann, and J. Edsjö, Phys. Rev. D **78**, 103520 (2008).

[12] T. Bringmann, X. Huang, A. Ibarra, S. Vogl, and C. Weniger, J. Cosmol. Astropart. Phys. 07 (**2012**) 054.

[13] L. Bergström, Phys. Rev. D **86**, 103514 (2012).

[14] B. Shakya, Phys. Dark Univ. **2**, 83 (2013).

[15] M. Garny, A. Ibarra, M. Pato, and S. Vogl, J. Cosmol. Astropart. Phys. 12 (**2013**) 046.

[16] G. Tomar, S. Mohanty and S. Rao, arXiv:1306.3646.

[17] T. Toma, Phys. Rev. Lett. **111**, 091301 (2013).

[18] F. Giacchino, L. Lopez-Honorez, and M. H. G. Tytgat, J. Cosmol. Astropart. Phys. 10 (**2013**) 025.

[19] N. F. Bell, J. B. Dent, T. D. Jacques, and T. J. Weiler, Phys. Rev. D **83**, 013001 (2011).

[20] N. F. Bell, J. B. Dent, T. D. Jacques, and T. J. Weiler, Phys. Rev. D **84**, 103517 (2011).

[21] P. Ciafaloni, M. Cirelli, D. Comelli, A. De Simone, A. Riotto, and A. Urbano, J. Cosmol. Astropart. Phys. 06 (**2011**) 018.

[22] N. F. Bell, J. B. Dent, A. J. Galea, T. D. Jacques, L. M. Krauss, and T. J. Weiler, Phys. Lett. B **706**, 6 (2011).

[23] M. Garny, A. Ibarra, and S. Vogl, J. Cosmol. Astropart. Phys. 07 (**2011**) 028.

[24] P. Ciafaloni, M. Cirelli, D. Comelli, A. De Simone, A. Riotto, and A. Urbano, J. Cosmol. Astropart. Phys. 10 (**2011**) 034.

[25] P. Ciafaloni, D. Comelli, A. De Simone, A. Riotto, and A. Urbano, J. Cosmol. Astropart. Phys. 06 (**2012**) 016.

[26] K. Fukushima, Y. Gao, J. Kumar, and D. Marfatia, Phys. Rev. D **86**, 076014 (2012).

[27] K. Shudo and T. Nihei, Phys. Rev. D **88**, 055019 (2013).

[28] M. Asano, T. Bringmann, and C. Weniger, Phys. Lett. B **709**, 128 (2012).

[29] M. Garny, A. Ibarra, M. Pato, and S. Vogl, J. Cosmol. Astropart. Phys. 11 (**2012**) 017.

[30] M. Garny, A. Ibarra, and S. Vogl, J. Cosmol. Astropart. Phys. 04 (**2012**) 033.

[31] L. Bergström, T. Bringmann, M. Eriksson, and M. Gustafsson, Phys. Rev. Lett. **95**, 241301 (2005).

[32] C. Garcia-Cely and A. Ibarra, J. Cosmol. Astropart. Phys. 09 (**2013**) 025.

[33] T. Bringmann, F. Calore, G. Vertongen, and C. Weniger, Phys. Rev. D **84**, 103525 (2011).

[34] M. Kachelriess and P. D. Serpico, Phys. Rev. D **76**, 063516 (2007).

[35] M. Kachelriess, P. D. Serpico, and M. A. .Solberg, Phys. Rev. D **80**, 123533 (2009).

[36] P. Ciafaloni and A. Urbano, Phys. Rev. D **82**, 043512 (2010).

[37] P. Ciafaloni, D. Comelli, A. Riotto, F. Sala, A. Strumia, and A. Urbano, J. Cosmol. Astropart. Phys. 03 (**2011**) 019.

[38] M. Cirelli, G. Corcella, A. Hektor, G. Hutsi, M. Kadastik, P. Panci, M. Raidal, F. Sala, and A. Strumia, J. Cosmol. Astropart. Phys. 03 (**2011**) 051; 10 (**2012**) E01.

[39] T. Hahn, Comput. Phys. Commun. **140**, 418 (2001).

[40] P. Gondolo, J. Edsjö, P. Ullio, L. Bergström, M. Schelke, and E. A. Baltz, J. Cosmol. Astropart. Phys. 07 (**2004**) 008; P. Gondolo, J. Edsjö, L. Bergström, P. Ullio, M. Schelke, E. A. Baltz, T. Bringmann, and G. Duda, Dark SUSY, http://www.darksusy.org.

[41] R. Mertig, M. Bohm and A. Denner, Comput. Phys. Commun. **64**, 345 (1991).

[42] J. Edsjö and P. Gondolo, Phys. Rev. D **56**, 1879 (1997).

[43] J. Edsjö, M. Schelke, P. Ullio, and P. Gondolo, J. Cosmol. Astropart. Phys. 04 (**2003**) 001.

[44] T. Bringmann, F. Calore, A. Galea, and M. Garny, (to be published).

[45] T. Sjöstrand, S. Mrenna, and P. Z. Skands, J. High Energy Phys. 05 (**2006**) 026.

[46] P. A. R. Ade *et al.* (Planck Collaboration), arXiv:1303.5076.

[47] Integrating Eq. (2) leads to a logarithmic divergence for $E_V \rightarrow 0$, which would be canceled by the contribution from loop corrections to the two-body annihilation process. Given the large values of m_Z and m_W, however, we only expect a very small impact of that effect in our case. Low-energy photons from $\bar{f}f\gamma$, on the other hand, are phenomenologically not important as they are always vastly dominated by secondary photons at the tree level [10]. Thus, we simply refer here to $(\sigma v)_{\bar{f}f\gamma}$ as the cross section into high-energy photons only, with $E_\gamma > 0.5m_\chi$.

[48] X. -l. Chen and M. Kamionkowski, J. High Energy Phys. 07 (**1998**) 001.

[49] C. E. Yaguna, Phys. Rev. D **81**, 075024 (2010).

[50] L. L. Honorez and C. E. Yaguna, J. High Energy Phys. 09 (**2010**) 046.

[51] A. Geringer-Sameth and S. M. Koushiappas, Phys. Rev. Lett. **107**, 241303 (2011); M. Ackermann *et al.* (Fermi-LAT Collaboration), arXiv:1310.0828.

[52] For neutralino models that could explain the monochromatic ~130 GeV signal around the galactic center [12,58] in terms of photon IB, on the other hand, the low-energy photon yield is never enhanced by more than a factor of ~2 (cf. Fig. 4 in Ref. [5]).

[53] C. Evoli, I. Cholis, D. Grasso, L. Maccione, and P. Ullio, Phys. Rev. D **85**, 123511 (2012).

[54] D. S. Akerib *et al.* (LUX Collaboration), arXiv:1310.8214.

[55] L. Bergström, T. Bringmann, and J. Edsjö, Phys. Rev. D **83**, 045024 (2011).

[56] S. Chatrchyan *et al.* (CMS Collaboration), Phys. Rev. Lett. **111**, 081802 (2013).

[57] ATLAS Collaboration, Report No. ATLAS-CONF-2013-041, 2013.

[58] C. Weniger, J. Cosmol. Astropart. Phys. 08 (**2012**) 007.